Study of Test Structures for Use as Reference Materials for Optical Critical Dimension Applications*

Richard A. Allen†, Heather J. Patrick‡,§§, Michael Bishop‡‡, Thomas A. Germer‡, Ronald Dixson§, William F. Guthrie††, and Michael W. Cresswell†

†Semiconductor Electronics Division
‡Optical Technology Division
§Precision Engineering Division
††Statistical Engineering Division
National Institute of Standards and Technology
Gaithersburg, Maryland 20899 USA

§§KT Consulting, Inc.
300 Wilbur Ave., Antioch, CA 94509

‡‡International SEMATECH Manufacturing Initiative
2706 Montopolis Drive
Austin, Texas 78741 USA

richard.allen@nist.gov

***Abstract*— Optical critical dimension (OCD) metrology has rapidly become an important technology in supporting the worldwide semiconductor industry. OCD relies on a combination of measurement and modeling to extract the average dimensions of an array of parallel features, having fixed pitch and drawn linwidth. This paper reports results of OCD measurements on arrays selected to serve as prototype reference structures. In addition, SEM CD measurements were made on several of these structures to verify line uniformity. These prototypes are fabricated using the single-crystal CD reference materials (SCCDRM) process, which in prior work has been successfully applied to isolated feature reference materials. The SCCDRM process provides features with known geometries, typically vertical sidewalls, defined by the silicon lattice.**

***Index Terms*—Metrology, Linewidth, Critical Dimension (CD), Optical Critical Dimension (OCD), Scatterometry**

I. Introduction

Optical critical dimension (OCD) metrology has rapidly become an important technology in supporting the worldwide semiconductor industry. OCD, also called scatterometry, is expected to be a key technology in current and future semiconductor manufacturing processes as cited in the most recent version of the International Technology Roadmap for Semiconductors.[1] OCD relies on a combination of measurement and modeling to extract the average dimensions of an array of parallel features, typically lines having equal drawn linewidth and pitch. This paper reports initial work at the National Institute of Standards and Technology (NIST) on developing reference materials for OCD applications. The reference materials under investigation are fabricated using the single-crystal CD reference materials (SCCDRM) process,[2] which provides features with known geometries—typically vertical sidewalls—defined by the silicon lattice.

Since the edges of features made using the SCCDRM process are silicon lattice-planes, the dimensions of any particular feature can be calibrated by using the known spacing of the silicon lattice (0.543 102 122(20) nm).[3,4] In addition, the geometry makes the SCCDRM excellent for use in atomic force microscopy (AFM) calibration and tip characterization.

Previous work focused on SCCDRM test structures with isolated features; calibration of these isolated features was for a single location on a particular feature.

OCD applications differ from conventional CD measurements in two critical ways:

- The CD is determined over a relatively large region: typically a spot size of 20 µm to 50 µm.
- Extraction of the CD depends on comparing an experimental signature to modeled signatures. The CD of the modeled signature that best matches the experimental signature is taken to represent the average CD of the lines in the grating test structure.

II. Grating Test Structure Design and Fabrication

The basic test structure consists of a grating target with adjacent isolated line test structures (Fig 1). Two sizes of grating targets were included on the first test chip. The targets are parallelograms so that all edges are aligned to the

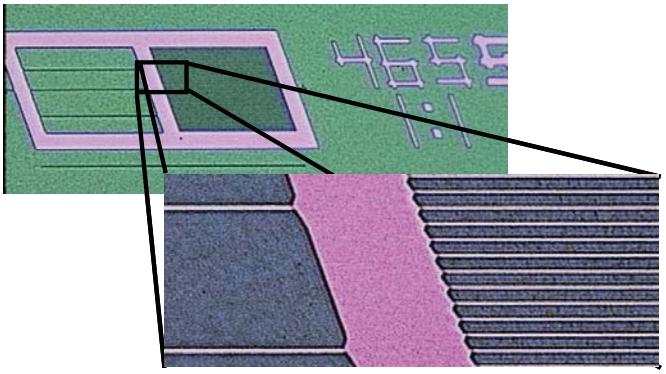

Fig. 1. Image of a single 100 µm OCD target showing detail of the grating as well as two of the adjacent isolated lines

* Contribution of the National Institute of Standards and Technology; not subject to copyright in the United States of America

1-4244-0781-8/07/$20.00 ©2007 IEEE

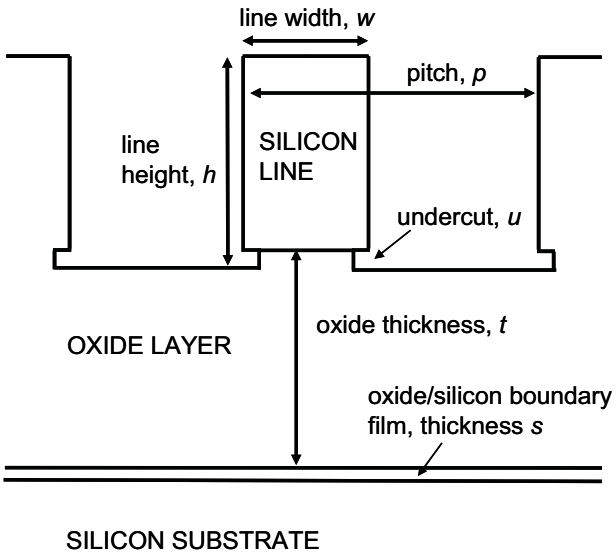

Fig. **2:** Line profile model used in RCW simulations of OCD signatures.

<112> lattice vectors in the silicon surface. Two sizes of targets were included in the design: the smaller targets measure 50 µm from top edge of the target to the bottom edge of the target while the larger targets measure 100 µm (note that all data in the paper were derived from 100 µm targets). The design widths of the lines in the grating targets range from 350 nm to 1000 nm; three grating target test structures were fabricated for each width. The individual structures were designed with a ratio of line width to line space of 1:1, 1:2, and 1:5. Adjacent to the grating test structure are several isolated features (of the same drawn dimension) as well as a limited number of navigation features.

OCD test structures were included on a test chip to be fabricated on a (110) SIMOX wafer. Use of a (110) SIMOX wafer provides features with a known height (i.e., the thickness of the SIMOX device layer) as well as vertical sidewalls defined by (111) silicon lattice planes.

The process used in the fabrication of these test structures[1] is based on the anisotropic etch techniques commonly found in microelectromechanical system (MEMS) production; upon completion, features with design dimensions of about 450 nm and greater were successfully transferred to the SIMOX device layer with a process bias (overetch) of 400 nm to 450 nm.

III. Optical Critical Dimension Measurement

A. Overview

In OCD, the parameters that best describe the lines of the target grating are determined by comparing measured optical signatures with simulated signatures generated from theory.[5,6,7] In the present work, the optical signatures consist of the reflectance of the grating at a fixed wavelength versus angle of incidence, measured for both s-polarization (the incident light is linearly polarized with E-field perpendicular to the plane of incidence) and for p-polarization (incident light linearly polarized with its E-field in the plane of incidence). The comparison is often made by generating a library of signatures and searching for the signature that best fits the data (the approach taken here),[6] or can be done using a nonlinear regression algorithm that varies the model parameters (such as line width, line height, and layer thickness) to minimize the

TABLE I. List of OCD targets used in this work

Target ID	P_{Design} *(nm)*	W_{Design} *(nm)*	W_{SEM} *(nm)*
00s 1:1	2000	1000	596
75s 1:1	1500	750	320
70s 1:1	1400	700	260
00s 1:2	3000	1000	595
70s 1:2	2100	700	301
55s 1:2	1650	550	125

Structures from chip identified as B1, Section 1:00. The printed pitch of the targets was equal to the design pitch p_{Design}, while significant etch bias caused printed target width (as estimated from SEM line width w_{SEM}) to be significantly smaller than the design width w_{Design}.

deviation between theoretical and experimental signatures.[4] The geometrical approximation chosen to represent the line shape, which we refer to here as the line profile model, is generally chosen to be the simplest structure that will adequately describe the grating and is necessarily an approximation to the actual line shape. The generation of theoretical signatures is computationally intensive. For example, for the line profile model used in this work, a library containing theoretical s- and p-polarized reflectance signatures for 10,000 combinations of model parameters required 260 processor-hours on a cluster computing system. Because of this, prior knowledge of the grating structure is used to determine reasonable ranges for the parameters of the line profile model. Advantages of OCD include speed, non-destructive measurement of the target, and ability to extract target dimensions that are much smaller than the wavelength of the incident light.

B. Data Acquisition

The measurement setup is shown in Figure 5. Light from a 532 nm laser is incident on the target at a variable angle of incidence θ. The light is focused on the target to a roughly Gaussian spot with a 20 µm full width at half maximum (FWHM). The laser polarization was set at either p- (E-field

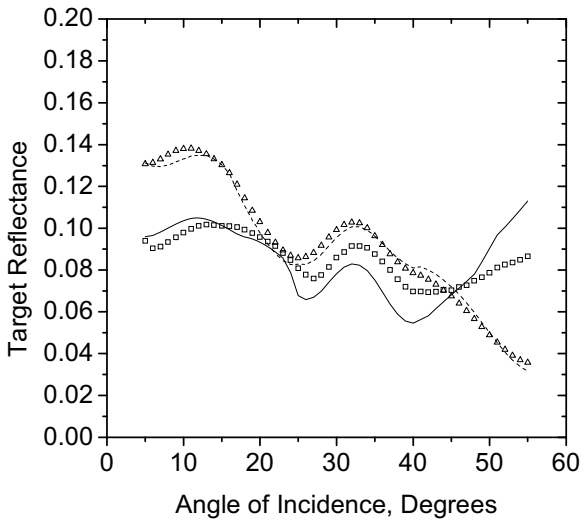

Fig. **3: Comparison of measured and simulated OCD signatures for s-polarization (squares: measured, solid line: simulated) and p-polarization (triangles: measured, dotted line: simulated), for the 75S 1:1 target. The simulated signatures shown are those with the best agreement to the data, out of a library of signatures generated using the line profile shown in Fig. 2, as discussed in the text.**

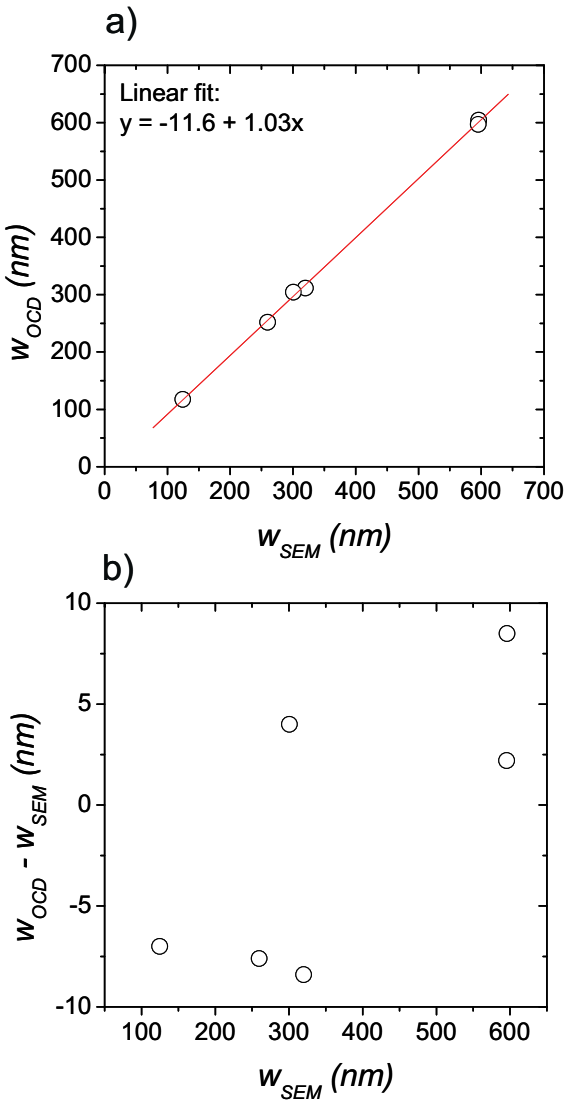

Fig. **4: a) CD line width extracted from OCD, *wOCD*, versus line width measured by SEM, *wSEM*, for six targets on SCCDRM chip B1. Each data point represents a different scatterometry target. b) Residual values of *w*OCD – wSEM for the data shown in a).**

in the plane of incidence) or s- (E-field perpendicular to the plane of incidence) polarization. The detector angle was maintained at twice the angle of incidence (2θ) so that the specular component of grating reflectance was collected, and θ was varied over a range of 5° to 55°. A small portion of the beam was picked off before the final focusing lens to provide a reference intensity measurement. The camera shown is used only for system alignment.

The s-polarization and p-polarization reflectance versus angle signatures were obtained for six targets in the 1:00 section of an SCCDRM chip identified as B1. The pitch, design line width, and average line width as measured by SEM of each target are shown in Table 1. Figure 3 shows example data from one of the grating test structures for s-polarization (squares) and p-polarization (triangles). The data were highly repeatable from day to day on the same target. Additionally, reference reflectance versus angle scans of a bare silicon wafer were taken periodically and compared with Fresnel theory in order to verify system operation. However, on OCD targets the data were seen to be sensitive to the quality of the focus spot at the target, as excess light

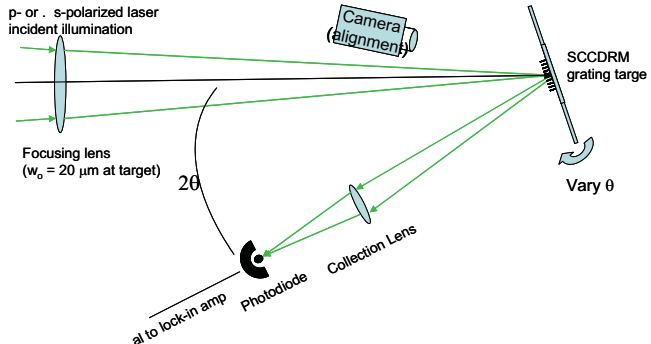

Fig. **5: Schematic of the data acquisition set-up for OCD signatures.**

that is incident on the chip outside of the intended target could be collected by the detector and introduce a systematic error into the signature. In the present case, the lens elements that determine the focus were fixed over the course of the data acquisition, and we believe we have minimized any defocus effects. Methods of further reducing the effects of stray light are being considered.

C. Theory

The simulated signatures were obtained using the rigorous coupled wave (RCW) analysis for surface relief gratings developed by Moharam *et al.*,[9,10] with a modification suggested by Lalanne and Morris[11] to improve the convergence of the calculations. This method solves the electromagnetic problem for a plane wave incident upon a medium having a dielectric function $\varepsilon(x,y,z) = \varepsilon_j(x)$, which is periodic in x, independent of y, and independent of z within each of a finite number of layers, indicated by index j. The solution requires Fourier series expansions of $\varepsilon_j(x)$ and $1/\varepsilon_j(x)$ for each layer. In practice, the Fourier series is truncated at some maximum order M, chosen here to be ±35. The model structure is shown in Fig. 2 and has six adjustable parameters: the grating pitch p, line height h, the linewidth w, the undercut u, the SiO_2 film thickness t, and a mixed SiO_2-Si boundary film thickness s. Since the sidewall angles are vertical, it was not necessary to include sidewall angle as an adjustable parameter. The undercut arises during etching of the chip and is modeled as a square region with height and width u. The complex indices of refraction of the materials ($n_{Si} = 4.143 + i0.0283$, $n_{oxide} = 1.5038$, $n_{mix} = 2.731 + i0.0128$ at the laser wavelength λ = 532 nm) were determined by spectroscopic ellipsometry on an unpatterned sample of SIMOX similar to that used for the SCCDRM chips. The value of n_{Si} used was the accepted value for silicon,[13] while the value of n_{oxide} was increased from typical values for bulk SiO_2 in order to improve the fit to the spectrosopic ellipsometry data. Differences in the optical properties of the SiO_2 layer in SIMOX wafers compared to that of bulk SiO_2 have been previously reported in the literature.[14] The boundary film n_{mix} was added ad hoc to improve the fits to the spectroscopic ellipsometry data; its thickness s = 11.4 nm was not varied when generating the libraries. This initial model of the substrate may not be unique, and other models (with additional layers, a graded interface between Si and SiO_2, etc.) may provide as good or better agreement with the optical data. The uncertainties in substrate parameters and the effect of these uncertainties on the OCD results are under investigation.

The general procedure for determining the target line parameters was as follows. The raw data consisted of the

measured reflectance of the grating, as a function of incidence angle, for s- and p-polarization as shown in Fig. 4. These data were compared with a library of simulated signatures for all combinations of the adjustable parameters over the selected range of those parameters, and the parameter set corresponding to the simulation having the minimum mean-square error (MSE) relative to the data was taken to be the best estimation of the parameters for the actual target. The MSE is given by[12]

$$MSE = \frac{1}{2N} \sum_{i=s,p} \sum_{j=1}^{N} [R_{meas,i}(\theta_j) - R_{sim,i}(\theta_j)]^2$$

where $N = 51$ is the number of discrete angles where the reflectance was measured, and the subscript i is used to denote that both s- and p-polarization reflectances were included in the MSE. The library generation is computationally intensive even when spread across multiple processors, so prior knowledge about the target was used to fix some parameters and to determine the ranges of others. The measured targets were all from the same chip, and only pitch and line width were expected to vary from target to target. The pitch p of each target was well known, so when producing a library for a given target, p was fixed to the value shown in Table 1 for that target. Likewise, the height of the targets was expected to be constant across the chip and was fixed to a value $h = 138$ nm, which was consistent with AFM measurements of nearby isolated lines. Of the remaining adjustable parameters, initial exploratory sets of six libraries (one for each target at the appropriate pitch) were produced where w was varied over a 200 nm range centered on w_{SEM} for the target, u was varied from 4 nm to 14 nm, and t was varied from 358 nm to 380 nm. The simulated signatures from the libraries were compared with the data, and for each target the parameter set corresponding to the simulation having the minimum mean-square error to the data was recorded. These results provided a approximate value of w for each target and indicated that, as expected, the values for t and u were consistent to within a few nm across the chip. A limited number of simulations were run where h was also allowed to vary; this did not significantly improve the agreement between data and simulation compared to the cases with fixed h. For our final estimation of the remaining free parameter w, we fixed $u = 11$ nm, $t = 366$ nm, and $h = 138$ nm for all of the targets, then generated a set of six libraries for w where, for each target, w was varied over a 20 nm range centered on its value from the exploratory libraries, in 0.5 nm steps. The simulated results were compared to the data, and the widths w corresponding to the simulations having the minimum mean-square error to the data are reported in Fig. 5.

IV. SEM CD Measurements

SEM CD measurements were made on a selection of test structures to

- Provide an independent measure of the CDs of the features in the array. Although the limitations of SEM CD are well understood, including not providing dimensional measures traceable to the ISO definition of the meter, it is widely used in semiconductor fabrication for process control for acquiring the relative CDs of features.
- Approximate the degree of line roughness for features in the array. This is done as a check since the OCD analysis assumes that there is no significant line edge roughness.

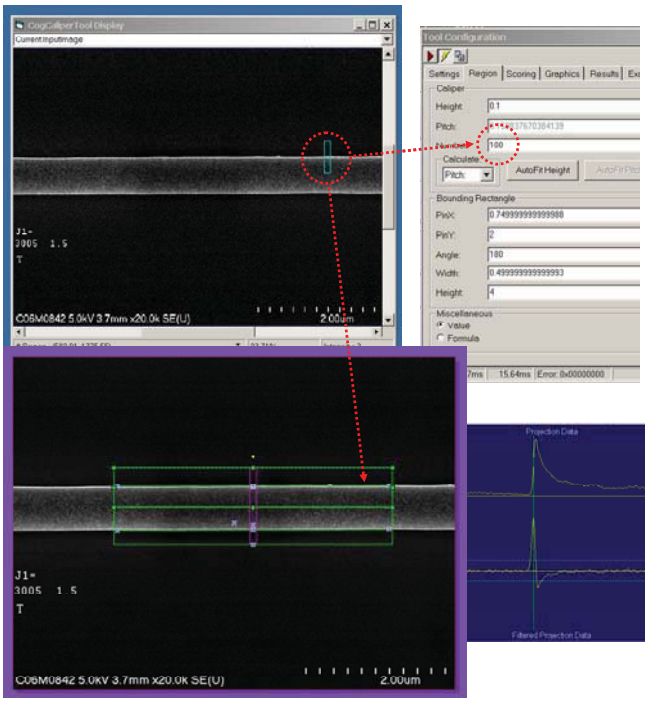

Fig. **6. Procedure for extracting the SEM CDs. The light blue measurement caliper is incremented 100 times through the region outlined by the green rectangle. 4 µm of each line was measured.**

SEM CD, however, is a significantly different measure than OCD in that the SEM images a relatively small area of the test structure.

Three SEM images were made in selected array test structures. Each of these images was captured at 20,000X at a resolution of 2560 pixels by 1920 pixels. Each of these images included 6.4 µm long sections of two or three line segments (depending on the line widths and spaces).

At this resolution, each image covers a region of 6.4 µm by 4.8 µm (30.72 µm^2). Therefore, the total area imaged by the SEM is 92.16 µm^2. In contrast, the OCD measurement averages the lines over much of the target area, in this case of 10,000 µm^2.

The dimensions of the lines in these images were determined automatically using the software package **IC3D**[†]**.** Using this technique the locations of each of the line edges was determined at 80 to 100 locations along the line. The edge roughness was estimated to range from 1.6 nm to 12.6 nm with an average value of 5.5 nm. Figure 6 shows the image analysis procedure used to acquire the width.

V. Results and Discussion

Figure 4 shows an example of the experimentally obtained reflectance signatures for s- and p-polarization on the 75s 1:1 target, and the final best fit simulated signatures obtained as described above. From this fit, we obtained a CD line width

[†] Certain commercial equipment, instruments, or materials are identified in this paper in order to specify the experimental procedure adequately. Such identification is not intended to imply recommendation or endorsement by the (NIST), nor is it intended to imply that the materials or equipment identified are necessarily the best available for the purpose.

w_{OCD} = 311.5 nm, which is in reasonable agreement with the average SEM line width w_{SEM} = 320 nm for this target. It can be seen in the figure that while the angular variations of the data were qualitatively reproduced by the best fit simulations, significant residual disagreement remained between the data and the simulation. This disagreement was seen, to varying degrees, for all of the targets and was not significantly reduced for any of the parameter combinations that were tried. The sources of this are under investigation and are expected to include deviations of the actual line profile from the simplified model, radiometric errors in the measurement due to imperfect laser focusing and reflections from areas outside the target being collected by the detector, and line variations across the target (including line roughness) that are not included in the model. In addition, the targets available to us in this study all had pitches greater than 1 μm, meaning that relatively few lines were illuminated by the 20 μm FWHM focused laser spot, while the RCW calculations assume that an infinite number of lines are illuminated.

Figure 5 a) shows the value of w_{OCD} determined for each of the six targets versus the average SEM linewidth, w_{SEM}, measured for that target. A straight-line model was fit to the data using linear regression with equal weight on each point, and the slope of w_{SEM} vs. w_{OCD} was found to be near 1, with a small offset, as shown in the figure. In Fig. 5 b), the difference between w_{OCD} and w_{SEM} has been plotted for each target. In all cases, the difference was less than 10 nm.

We wish to compare the uncertainties in the residuals plotted in Fig. 5 b) with the uncertainties in w_{SEM} and w_{OCD}. The typical standard uncertainty in w_{SEM} (the average line width of the target) was ± 2.5 nm, although local variations of line width across the target could be 2 to 3 times this value. The component of the uncertainty in w_{OCD} due to the repeatability of the reflectance signatures was estimated as follows. For one target on another SCCDRM chip (distinct from chip B1 but from the same wafer), reflectance data were taken on 4 separate days, with the chip removed and replaced into the sample holder each day. The resulting reflectance data sets were fit to a library where the parameters *t, u,* and *w* were allowed to vary, with step sizes of 0.5 nm, 0.5 nm, and 0.2 nm, respectively. Although slight differences could be seen in the optical signatures from day to day, the standard deviation of w_{OCD} over the 4 data sets was only 0.4 nm. We do not believe that the repeatability of the reflectance measurement is the only source of error in w_{OCD}, however. As this work progresses, one of our goals is to carry out a more comprehensive uncertainty analysis to quantify a range of model parameters, including w_{OCD}, that are consistent with the data for each target. The current level of disagreement between simulation and data for each target (as seen in Fig. B) makes this difficult.

We are nonetheless encouraged by the results from this exploratory study. While the differences between w_{OCD} and w_{SEM} are not completely accounted for by known sources of uncertainty at this point, we observed excellent correlation between the two techniques, with unity slope and very little offset between the line width measured by SEM and that extracted from the OCD simulations. We believe this is due in part to the 90° sidewall angle of the silicon lines. In OCD targets with non-perpendicular sidewalls, cross-coupling between line width and sidewall angle in the optical signature is often a significant source of uncertainty in line width measurement.[8] In the current case, this source of uncertainty was not present. It should be noted that, to some degree, the simplicity afforded by the perpendicular grating sidewalls is offset by the noted complexity of the substrate modeling, where a boundary layer between Si and SiO_2 appears to be present and where the thickness of the SiO_2 layer is a model parameter. Improved characterization of the substrate and the effect of substrate parameters on the OCD results are being considered.

VI. Conclusions

Successful development of standards for OCD will depend on solving several key issues. The first is that OCD accuracy should be separated into model accuracy and radiometric accuracy. Model accuracy depends on both well-developed signatures and the quality of fit of the unknown signature. Validation of models may depend on standard profiles generating known, accepted signatures. Radiometric accuracy can be addressed with artifacts to check the consistency of instrument measurements. These artifacts could include both a grating structure, such as described in this paper, as well as artifacts that are already available (e.g., ellipsometry standards for ellipsiometric angles Ψ and Δ, reflectance standards). Preliminary results from grating test structures presented in this paper will be used by NIST to determine the best path for developing reference materials for this technology.

Acknowledgments

We thank L. Richter of NIST for assistance with spectroscopic ellipsometry measurements and the NIST Office of Microelectronics Programs for supporting this work. H. J. Patrick and T. A. Germer acknowledge the use of the NIST Raritan cluster system.

References

[1] http://www.itrs.net/Links/2005ITRS/Metrology2005.pdf, p. 8, 20

[2] M.W. Cresswell, W.F. Guthrie, R.G. Dixson, R.A. Allen, C.E; Murabito, and J. V. Martinez De Pinillos., "RM 8111: Development of a Prototype Linewidth Standard" J. Res. Natl. Inst. Stand. Technol. 111, 187-203 (2006).

[3] R.A. Allen, T.J. Headley, S.C. Everist, R.N. Ghoshtagore, M.W. Cresswell, and L. W. Linholm, High-resolution transmission electron microscopy calibration of critical dimension (CD) reference materials, IEEE Trans. Semiconduct. 14(1), 26-31 (2001).

[4] P. J. Mohr and B. N. Taylor, CODATA recommended values of the fundamental physical constants: J. Phys. Chem. Ref. Data 28(6), 1713-1852 (1999). This paper was also published in Rev. Mod. Phys. 72 (2), 351-495 (2000). The values of these constants are also available online at physics.nist.gov/constants.

[5] C. J. Raymond, M. R. Murnane, S. L. Prins, S. S. H. Naqvi, and J. R. McNeil, "Multiparameter grating metrology using optical scatterometry," J. Vac. Sci. Technol. B, **15**, 361-368 (1997).

[6] A. Levy, S. Lakkapragada, W. Mieher, K. Bhatia, U. Whitney, and M. Hankinson, "Spectroscopic CD Technology or Gate Process Control," *The 2001 IEEE Semiconductor Manufacturing Symposium,* p. 141-144 (2001).

[7] W. Yang, J. Hu, R. Lowe-Webb, R. Kohlahalli, D. Shivaprasad, H. Sasano, W. Liu, and D. S. L. Mui, "Line-Profile and Critical-Dimension Monitoring Usinga Normal Incidence Optical CD Metrology," IEEE Transactions on Semiconductor Manufacturing, **17**, 564-572 (2004).

[8] R. Quintanhila, J. Hazart, P. Thony, and D. Henry, "Application of spectroscopic scatterometry method in hole matrices analysis," in

Metrology, Inspection, and Process control for Microlithography XIX, R.M.Silver, Ed., Proc. SPIE 5752, 204-216, (2005).

[9] M. G. Moharam, E. B. Grann, D. A. Pommet, and T. K. Gaylord, "Formulation for stable and efficient implementation of the rigorous coupled-wave analysis of binary gratings," J. Opt. Soc. Am. A 12, 1068-1076 (1995).

[10] M. G. Moharam, D. A. Pommet, E. B. Grann, and T. K. Gaylord, "Stable implementation of the rigorous coupled-wave analysis for surface-relief gratings: enhanced transmittance matrix approach," J. Opt. Soc. Am. A 12, 1077-1086 (1995).

[11] P. Lalanne and G. M. Morris, "Highly improved convergence of the couple-wave method for TM polarization," J. Opt. Soc. Am. A 13, 779-784 (1996).

[12] G. E. Jellison, Jr., "Data analysis for spectroscopic ellipsometry," Thin Solid Films **234**, 416-422 (1993).

[13] C. M. Herzinger, B. Johs, W. A. McGahan, J. A. Woolam and W. Paulson, "Ellipsometric determination of optical constants for silicon and thermally grown silicon dioxide via a multi-sample, multi-wavelength, multi-angle investigation," J. Appl. Phys. **83**, 3323-3336 (1998).

[14] B. J. Mrstik, P. J. McMarr, R. K. Lawrence and H. L. Hughes, "The use of spectroscopic ellipsometry to predict the radiation response of SIMOX", IEEE Trans. on Nuclear Science, **41**, 2277-2283 (1994).